KINEMATICS, DYNAMICS AND CONSTRUCTION OF A PLANARLY ACTUATED PARALLEL ROBOT

Ronen Ben-Horin[1], Moshe Shoham[1] and Shlomo Djerassi[2]

[1]Department of Mechanical Engineering
Technion - Israel Institute of Technology
Technion City, Haifa 32000, Israel
E-mail: shoham@tx.technion.ac.il
[2]RAFAEL - P.O.Box 2250 Haifa, Israel

ABSTRACT

Kinematic and dynamic analysis of a parallel robot consisting of three planarly-actuated links, is presented in this paper. Coordinated motion of three planar motors, connected to three fixed-length links, produces a six-degrees-of-freedom motion of an output link. Its extremely simple design along with much larger work volume than the commonly used parallel robots make this high performance-to-simplicity ratio robot very attractive. Experimental model verifies the unique combination of large work volume and high accuracy of this robot.

1. INTRODUCTION

The kinematic structure of most contemporary robots is an open kinematic chain structure (known also as serial manipulators or anthropomorphic structure). Only relatively few commercial robots are composed of a closed kinematic chain (parallel) structure. However, the increasing interest in parallel robots points to the potential embedded in this structure which has not yet been fully exploited. The advantages of parallel robots as compared to serial ones are:

- higher payload-to-weight ratio since the payload is carried by several links in parallel,
- higher accuracy due to non-cumulative joint error,
- higher structural rigidity, since the load is usually carried by several links in parallel and in some structures in compression-traction mode only,
- location of motors at or close to the base,
- simpler solution of the inverse kinematics equations.

Conversely, they suffer from smaller work volume, singular configurations and a more complicated direct kinematic solution (which is usually not required for control purposes).

A six degrees-of-freedom parallel manipulator was introduced by Stewart in 1965 [Stewart, 1965] and since then has been commonly known as the "Stewart-platform". (It appears that much earlier versions of parallel manipulators were already studied, see [Merlet, 1994]). Many variants of this structure have since been investigated; most of them are configurations having six linearly actuated links with different combinations of link-platform connections such as 3-3, 3-6, and the more general 6-6 one (see Fig. 1). Examples of different structures of parallel manipulators are given in [Chen and Song, 1992; Hunt, 1983; Innocenti and Parenti-Castelli, 1991,1994; Lin et al., 1990,1992; Pierrot et al., 1991; Waldron et al., 1989]. An atlas of parallel robots was composed by Merlet and can be found in the web site [http:// www.inria.fr/ prisme/ personnel/ merlet/ merlet_eng.html].

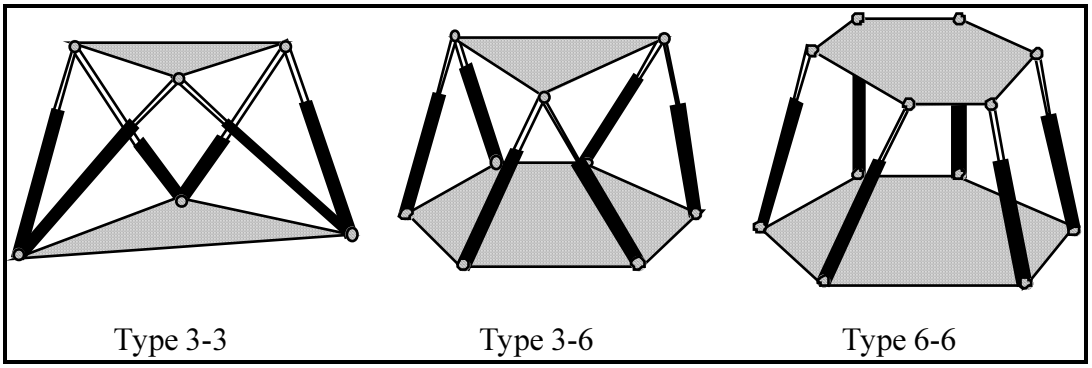

Fig. 1: Stewart platform type 3-3, 3-6, 6-6

This paper analyses a different type of a parallel manipulator that takes advantage of two-degrees-of-freedom planar motors. Coordinated motion of three such planar motors is converted through a spatial mechanism with fixed length links, into a six-degrees-of-freedom motion of the output link. Such a mechanism has many advantages over the common six extendible links parallel manipulators. It has a much larger work volume, very simple forward and inverse kinematic solutions, and it contains only seven moving parts (including motors) and six joints without any gear trains, cables or other power transmission devices. Thus, this robot is probably the simplest six degrees-of-freedom type robot (both parallel and serial) [Tsai and Tamahshebi, 1993; Ben-Horin and Shoham, 1996].

In this paper the kinematic and dynamic analysis of this robot is presented. The dynamic simulation also compares its performance with the common Stewart platform parallel robot. The experimental model, which to the best of our knowledge is the first

one that has been actually built, exhibits the unique combination of accuracy and work volume of this robot type.

The manipulator, shown in Fig. 2, consists of the following components: three links of fixed length having a spherical joint on one end and a revolute joint on the other end, three actuators which move planarly on a stationary platform and a six-degrees-of-freedom output platform.

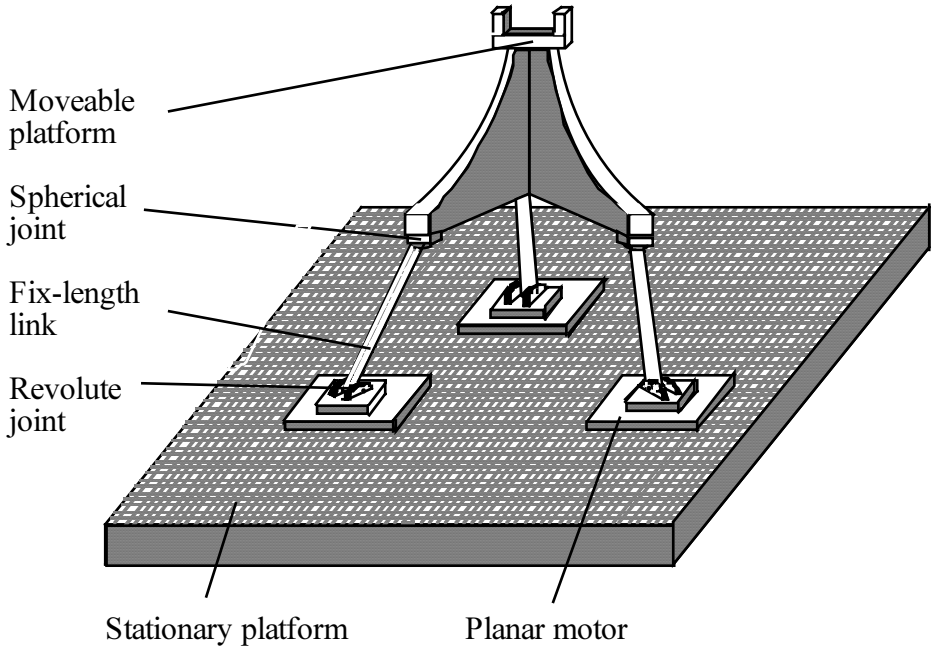

Fig. 2: A six-degrees-of-freedom parallel manipulator with three planarly actuated links.

2. MANIPULATOR KINEMATICS

2.1 Solution of the inverse kinematics

Manipulation tasks are usually given as a set of positions and orientations in world coordinate system of the robot's end-effector trajectory. To achieve these tasks it is necessary to transform the end-effector trajectory into active joints motion. This transformation, known also as the inverse kinematic problem, is, in our case, the calculation of the position of the three planar motors from a given position and orientation of the moveable platform.

This section describes the solution of the inverse kinematics which, as is usually the case with typical parallel manipulators, is simpler than the forward kinematics (see Section 2.2).

Define a coordinate system N attached to the stationary platform such that the $\mathbf{n}_3$ axis is normal to the platform. Define another coordinate system, K attached to the moving platform such that the $\mathbf{k}_3$ axis is normal to the moving platform (see Fig. 3).

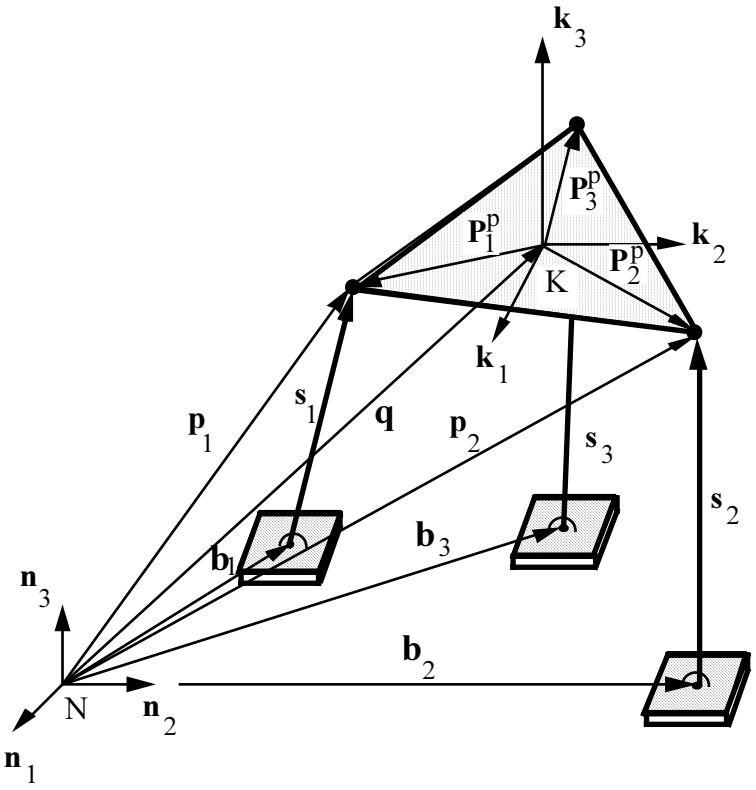

Fig. 3: Kinematic skeleton of the manipulator

If $\mathbf{p_i}$ is the position vector from origin N to spherical joint i, and $\mathbf{b_i}$ is the position of motor i (intersection of link i with motor i), then the following relation exists:

$$\mathbf{p}_i = \mathbf{s}_i + \mathbf{b}_i \tag{1}$$

where $\mathbf{s_i}$ is the vector of link i and given, with respect to N, by:

$$\mathbf{s}_i = \begin{bmatrix} l_i \cos\beta_i \cos\alpha_i \\ l_i \cos\beta_i \sin\alpha_i \\ l_i \sin\beta_i \end{bmatrix} \tag{2}$$

l_i is the length of link i with elevation and yaw angles α_i ,β_i as shown in Fig. 4.

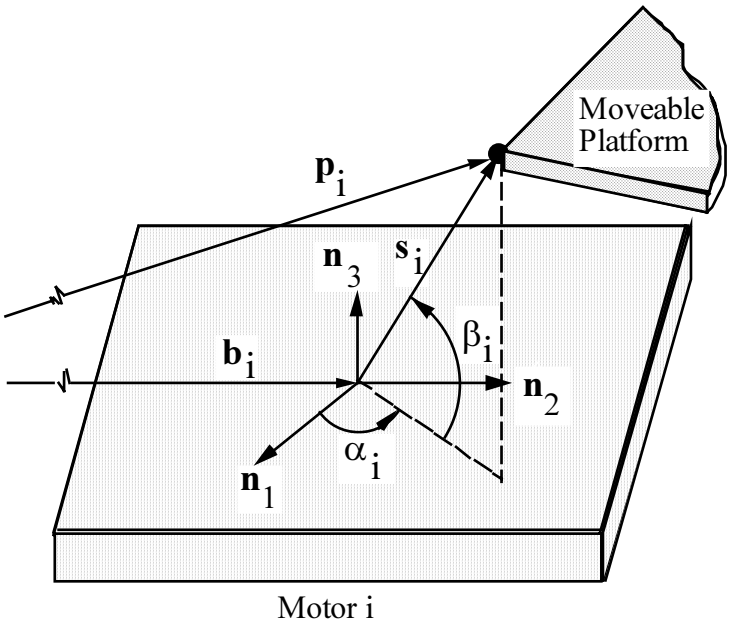

Fig. 4: link's parameters

Vector $\mathbf{p_i}$ can be calculated from the known constant positions of the spherical joints relative to the moving coordinate system, $\mathbf{p}_i^p$, and the required given position, **q**, and orientation, **R**, of the moving coordinate system.

$$\mathbf{p}_i = \mathbf{q} + \mathbf{R}\mathbf{p}_i^p \tag{3}$$

Solving Eq. (1) for the position of the planar motors, $\mathbf{b_i}$, gives the coordinate of the motors in N:

$$b_{i,1} = p_{i,1} - l_i \cos\beta_i \cos\alpha_i \tag{4}$$

$$b_{i,2} = p_{i,2} - l_i \cos\beta_i \sin\alpha_i \tag{5}$$

where

$$\beta_i = \sin^{-1}\frac{p_{i,3} - b_{i,3}}{l_i} \tag{6}$$

Using this inverse kinematics solution, it is possible to calculate the motors motion needed to achieve a given moveable platform (output link) trajectory. Fig. 5a shows the motor's motions on the stationary plate to achieve a $\pi/2$ rotation about the z axis. (The starting position is mark with a small circle). In Fig. 5b the same moveable platform motion is combined with a 200 mm translation along the x axis (see Section 7 for actual robot's dimensions).

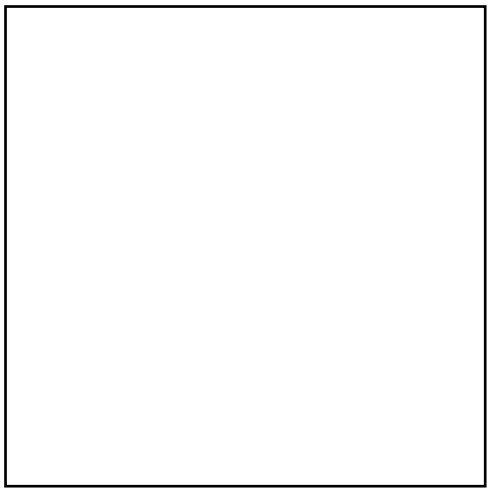

Fig. 5a

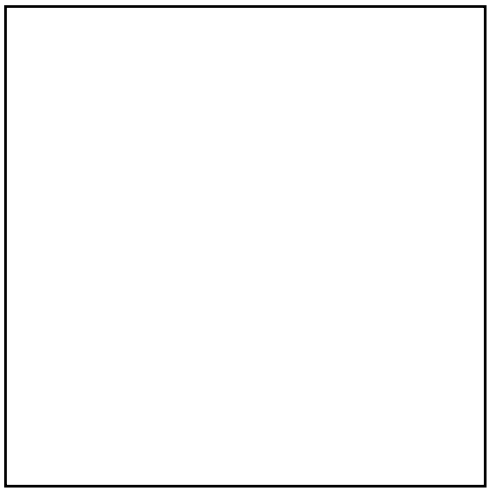

Fig. 5b

Fig. 5: Motors' paths for rotation and translation of the moveable platform.

2.2 Solution of the Direct Kinematics

The direct kinematics calculates the position and orientation of the moveable platform from a given position of the planar motors. Our solution follows the same path of Nanua et. al. [1990] but the resulting solution is simpler since firstly, only three rather than six links are involved in the present mechanism and secondly, the motion of the motors is a planar one.

The solution given by Tahmasebi and Tsai [1994] differs from the one given below because of a different order of joints. In Tahmasebi and Tsai's solution the spherical joints are close to the base and the revolute joints are on the distal end, while in the present design the order is reversed. It should be mentioned that this type of robot differs from the conventional fix-link's end-position parallel robots where each one of the platforms can be considered either the stationary or the movable one. Inverting the spherical and the revolute joints does yield, in our case, a different solution of the kinematics.

Assuming a rigid moveable platform, then the distance between two spherical joints, i and j, is a constant, a_{ij}

$$\left|\mathbf{p}_j - \mathbf{p}_i\right| = a_{ij} \qquad i, j = 1, 2, 3 \qquad i \neq j \tag{9}$$

Substituting for the magnitude of $\mathbf{p}_i$, the above equation becomes:

$$\begin{aligned} &(x_j - x_i + l_j \cos\beta_j \cos\alpha_j - l_i \cos\beta_i \cos\alpha_i)^2 + \\ &(y_j - y_i + l_j \cos\beta_j \sin\alpha_j - l_i \cos\beta_i \sin\alpha_i)^2 + \\ &(z_j - z_i + l_j \sin\beta_j - l_i \sin\beta_i)^2 - a_{ij} = 0 \end{aligned} \tag{10}$$

which can be written as a function of the unknown β_i as:

$$\begin{aligned} &D_1 \cos\beta_j + D_2 \cos\beta_i + D_3 \cos\beta_j \cos\beta_i + \\ &D_4 \sin\beta_j + D_5 \sin\beta_i + D_6 \sin\beta_j \sin\beta_i + \\ &D_7 = 0 \end{aligned} \tag{11}$$

where:

$$\begin{aligned} D_1 &= 2\Delta x A_j + 2\Delta y B_j \\ D_2 &= -2\Delta x A_i - 2\Delta y B_i \\ D_3 &= -2A_j A_i - 2B_j B_i \\ D_4 &= 2\Delta z l_j \\ D_5 &= -2\Delta z l_i \\ D_6 &= -2l_j l_i \\ D_7 &= \Delta x^2 + \Delta y^2 + \Delta z^2 + l_j^2 + l_i^2 - a_{ij}^2 \end{aligned}$$

and

$$\begin{aligned} \Delta x &= x_j - x_i \\ \Delta y &= y_j - y_i \\ \Delta z &= z_j - z_i \\ A_j &= l_j \cos\alpha_j \\ A_i &= l_i \cos\alpha_i \\ B_j &= l_j \sin\alpha_j \\ B_i &= l_i \sin\alpha_i \end{aligned}$$

Substituting the tangent half angle form into the above equation and casting the unknown β_i into the known terms the following equation is obtained:

$$I_2 t_j^2 + I_1 t_j + I_0 = 0 \tag{12}$$

where:

$$\begin{aligned} I_0 &= (D_1 - D_2 - D_3 + D_7)t_i^2 + 2D_5 t_i + D_1 - D_2 - D_3 + D_7 \\ I_1 &= 2D_4 t_i^2 + 4D_6 t_i + 2D_4 \\ I_2 &= (-D_1 - D_2 + D_3 + D_7)t_i^2 + 2D_5 t_i - D_1 + D_2 - D_3 + D_7 \end{aligned}$$

and

$$t_i = \tan\frac{\beta_i}{2}$$

Note that if we consider the unknown β_i as part of the known term I_i, then it results in three uncoupled quadratic equations,

$$\text{for} \quad i=1, j=2 \qquad E_2 t_2^2 + E_1 t_2 + E_0 = 0 \tag{13}$$

$$\text{for} \quad i=3, j=2 \qquad G_2 t_2^2 + G_1 t_2 + G_0 = 0 \tag{14}$$

$$\text{for} \quad i=1, j=2 \qquad H_2 t_2^2 + H_1 t_2 + H_0 = 0 \tag{15}$$

where E_i, G_i, and H_i are functions of the unknown variable t_1,t_3, and t_1 respectively.

The solution of this non-linear system of equations is obtained by [Salmon, 1964]:

$$\begin{vmatrix} G_2 & G_1 \\ E_2 & E_1 \end{vmatrix} \begin{vmatrix} G_2 & G_0 \\ E_2 & E_0 \end{vmatrix} - \begin{vmatrix} G_0 & G_2 \\ E_0 & E_2 \end{vmatrix} \begin{vmatrix} G_0 & G_1 \\ E_0 & E_1 \end{vmatrix} = 0 \tag{16}$$

which results in a fourth order polynomial in t_1 and t_3.

Rearranging terms and eliminating t_1,

$$J_4 t_3^4 + J_3 t_3^3 + J_2 t_3^2 + J_1 t_3 + J_0 = 0 \tag{17}$$

where J_i, i=0-4, are functions of only t_3.

Applying again the above method for Eqs. (15) and (17), both of which are functions of t_1 and t_3,

$$\begin{vmatrix} (J_3H_2 - J_4H_1) & (J_2H_2 - J_4H_0) & J_1H_2 & J_0H_2 \\ (J_2H_2 - J_4H_0) & (J_2H_1 - J_3H_0 + J_1H_2) & (J_1H_1 + J_0H_2) & J_0H_1 \\ H_2 & H_1 & H_0 & 0 \\ 0 & H_2 & H_1 & H_0 \end{vmatrix} = 0 \tag{18}$$

a sixteenth order polynomial in t_1 is obtained.

This polynom contains only even powers of t_1 hence two sets of eight reflected solutions exist. Among them we are interested in the real and positive solutions only. Knowing t_1, t_2 and t_3 are then calculated from the quadratic Eqs. (13) and (15) while Eq. (14) is used to examine the validity of the solution. An example of four solutions for a given position of the motors is shown in Fig. 6. The other four are reflected about the stationary platform.

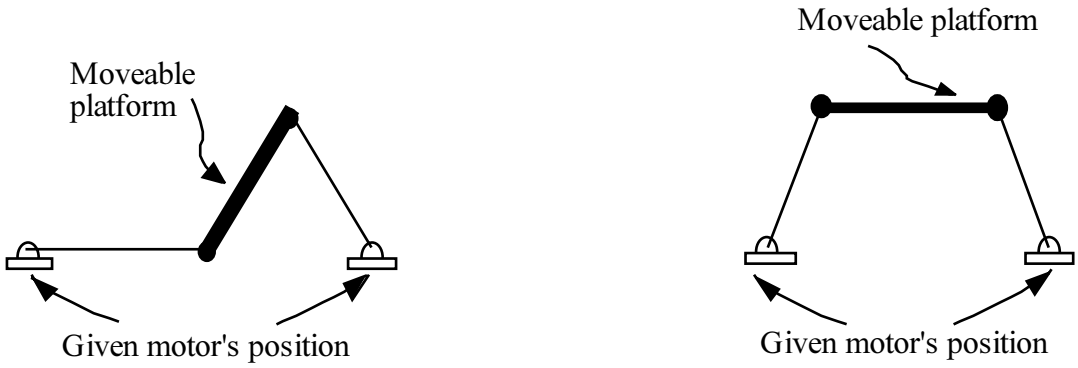

Fig 6: Four solutions for a given motors' position

5. MANIPULATOR DYNAMICS

Since the late eighties the dynamic of parallel robots has been investigated in several papers. Do and Yang [1988] introduced an algorithm to solve the inverse dynamics for platform type of manipulators using Newton-Euler equations of motion. They found that the inverse dynamics of the system is governed by thirty-six linear equations. The number of these simultaneous equations can be reduced to six, if a proper sequence is taken. Zhang and Song [1993] presented a more computationally efficient scheme based on the virtual work principle for inverse dynamics of a general Stewart platform. Gosselin [1996] proposed a parallel computational algorithm for the kinematics and dynamics of planar and spatial parallel manipulators. He showed that, for this type of manipulator, the inverse kinematics and the inverse dynamics procedures can be easily parallelized. The result is a closed-form efficient algorithm, based on Newton-Euler formalism, using n processors, where n is the number of kinematic chains connecting the base to the end-effector. Pang and Shahinpoor [1994] introduced an algorithm to solve the inverse dynamics of parallel manipulator based on Lagrangian technique. They showed that one should introduce and subsequently eliminate Lagrange multipliers to arrive at the governing equations. Zhiming [1994] showed that special features of the Stewart platform can lead to decomposition of the moving platform and the legs in the dynamics analysis. With this decomposed formulation, one can investigate the effect of leg inertia to determine whether such effect should be included in the actual implementation of control strategy, and use this formulation to implement control algorithm when the effect of leg inertia can not be neglected.

Our analysis employs Kane's equations to develop a parallel robot dynamics in a general form. A recent publication that employs Kane's equations to a specific parallel robot dynamics can be found in Baiges and Duffy [1996]. This general representation allows us first, to obtain the solution of different types of parallel robots in a simple way and secondly, to obtain a set of equations from which both the inverse and the forward

dynamics can be easily derived. We apply and simulate the results of four types of robots: two variations of the planarly actuated robot described in this paper, and for a comparison purposes the known 3-3 and 3-6 Stewart platforms.

5.1 Dynamics of the planarly actuated manipulator

The dynamics of the planary actuated manipulator is developed in this section. First the inverse dynamics is derived i.e., given the required trajectory of the moving platform, the motor forces are calculated. Next, the forward dynamics is derived, i.e. given the forces applied at the motors the moving platform trajectory is then calculated. For both cases the AUTOLEV dynamic package was used to determine the dynamic equations and to simulate the manipulator motion.

The dynamic model of the robot is shown in Fig 7.

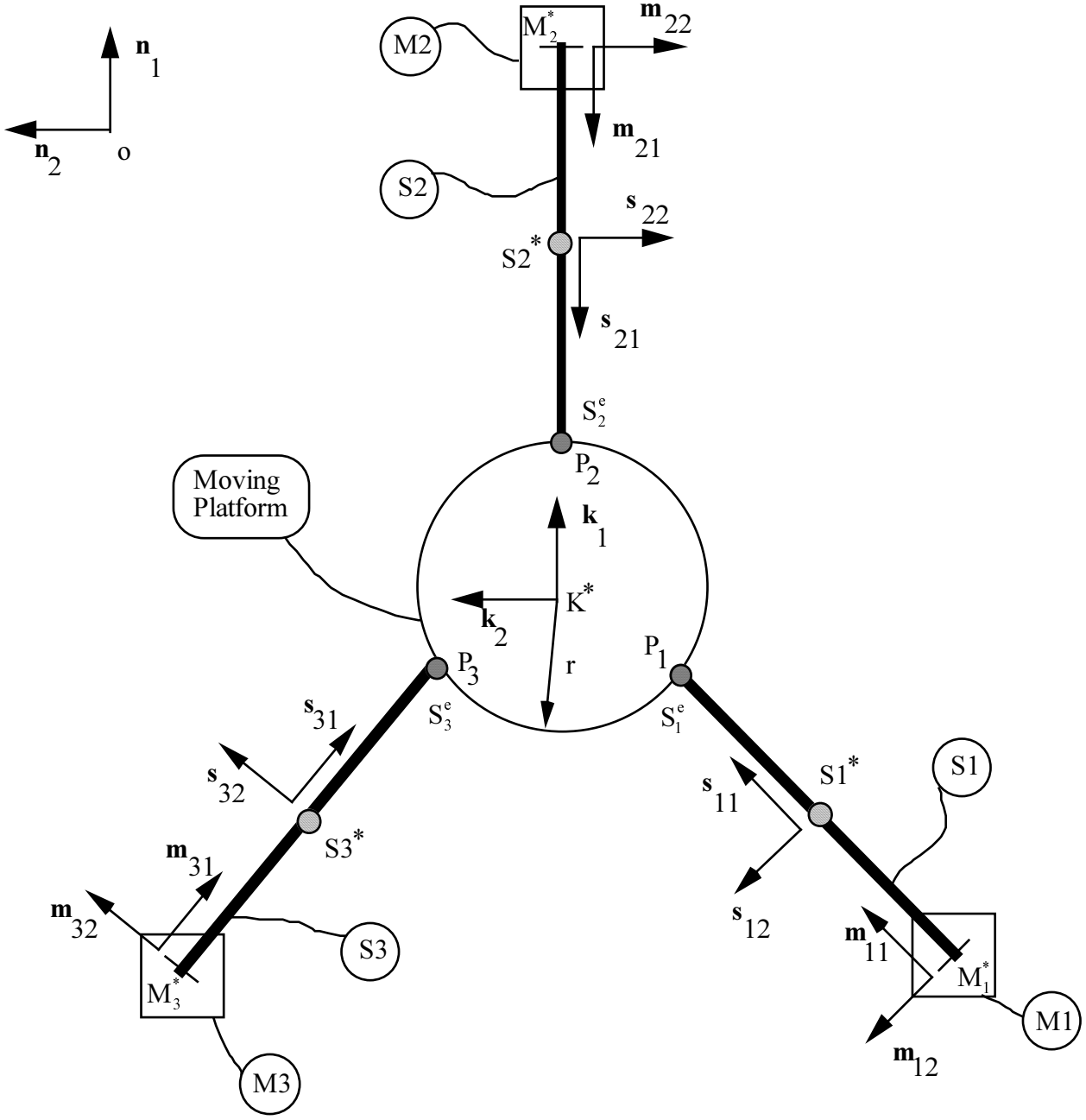

Fig 7: The dynamic model of the planarly actuated robot

The system consists of a moving platform K attached at points P_i (i=1,2,3) to the end points S_i^e of uniform, cylindrical rods S_i (i=1,2,3) respectively, by means of ball joints, symmetrically located on a circle of radius r fixed in the moving platform. The rods S_i are attached to bodies M_i (i=1,2,3) by means of revolute joints, whose axes are fixed in both S_i and in M_i, and cross M_i at their center of mass M_i^*. Finally, the mass center of the moving platform, K^*, coincides with the center of the circle derived by P_i; S_i^*. The mass centers of S_i are located at the midspan of S_i; and M_i^* remain in plane PL fixed in N at all times.

Let $\mathbf{n}_i$, $\mathbf{k}_i$, $\mathbf{s}_{ij}$ (i,j = 1, 2, 3) be sets of three dextral, mutually perpendicular unit vectors fixed in stationary, moving platforms and S_i respectively, and oriented as in Fig. 7. Also, let $\mathbf{s}_{i1}$ be aligned with the vectors $\mathbf{s}_i$ of the centerlines of S_i and let $\mathbf{s}_{i2}$, $\mathbf{n}_1$ and $\mathbf{n}_2$ all be parallel to plane PL. Finally, let $\mathbf{m}_{i1}$ (i = 1, 2, 3) be three unit vectors parallel to PL and aligned with the projection of the centerlines of S_i on PL; and let O be the origin of N.

Now, the configuration of the system in N can be described with the aid of fifteen coordinates, defined as follows:

$$q_i \triangleq \mathbf{p}^{OM_1^*} \cdot \mathbf{n}_i \qquad (i = 1,2) \tag{19}$$
$$q_3 \triangleq \cos^{-1}(\mathbf{s}_{11} \cdot \mathbf{m}_{11}) \tag{20}$$
$$q_i \triangleq \mathbf{p}^{OM_2^*} \cdot \mathbf{n}_{i-3} \qquad (i = 4,5) \tag{21}$$
$$q_6 \triangleq \cos^{-1}(\mathbf{s}_{21} \cdot \mathbf{m}_{21}) \tag{22}$$
$$q_i \triangleq \mathbf{p}^{OM_3^*} \cdot \mathbf{n}_{i-6} \qquad (i = 7,8) \tag{23}$$
$$q_9 \triangleq \cos^{-1}(\mathbf{s}_{31} \cdot \mathbf{m}_{31}) \tag{24}$$
$$q_i \triangleq \mathbf{p}^{OK^*} \cdot \mathbf{n}_{i-9} \qquad (i = 10,11,12) \tag{25}$$

The three last coordinates q_{13}, q_{14} and q_{15} are chosen to be space 1-2-3 rotation angles [Kane, 1983], describing the orientation of K in N.

The approach chosen here to describe the motion of the system in N is as follows: the ball joints attaching the moving platform to the limbs S_i are temporarily removed, so that the moving platform is regarded as undergoing an unconstrained motion (thus, the velocities of points P_i differ from those of points S_i^e, respectively). This unconstrained motion can be described with the aid of fifteen generalized speeds, defined as follows:

$$u_i \triangleq \mathbf{v}^{M_1^*} \cdot \mathbf{n}_i \quad (i = 1,2) \tag{26}$$
$$u_3 \triangleq -\omega^{S_1} \cdot \mathbf{m}_{12} \tag{27}$$
$$u_i \triangleq \mathbf{v}^{M_2^*} \cdot \mathbf{n}_{i-3} \quad (i = 4,5) \tag{28}$$
$$u_6 \triangleq -\omega^{S_2} \cdot \mathbf{m}_{22} \tag{29}$$
$$u_i \triangleq \mathbf{v}^{M_3^*} \cdot \mathbf{n}_{i-6} \quad (i = 7,8) \tag{30}$$
$$u_9 \triangleq -\omega^{S_3} \cdot \mathbf{m}_{32} \tag{31}$$
$$u_i \triangleq \mathbf{v}^{K^*} \cdot \mathbf{n}_{i-9} \quad (i = 10,11,12) \tag{32}$$
$$u_i \triangleq \omega^K \cdot \mathbf{k}_{i-12} \quad (i = 13,14,15) \tag{33}$$

The associated kinematical equations are:

$$\dot{q}_i = u_i \quad (i = 1,\ldots,12) \tag{34}$$
$$\dot{q}_{13} = u_{13} + \tan q_{14}(u_{14} \sin q_{13} + u_{15} \cos q_{13}) \tag{35}$$
$$\dot{q}_{14} = u_{14} \cos q_{13} - u_{15} \sin q_{13} \tag{36}$$
$$\dot{q}_{15} = (u_{14} \sin q_{13} + u_{15} \cos q_{13}) / \cos q_{14} \tag{37}$$

Moreover, the definitions in Eqs. (26) - (33) enable one to express the velocities of K^*, M_i^*, and S_i^*, and the angular velocities of K, M_i, and S_i as

$$\omega^{M_1} = 0, \quad \mathbf{v}^{M_1^*} = u_1\mathbf{n}_1 + u_2\mathbf{n}_2 \tag{38}$$

$$\omega^{S_1} = -u_3\mathbf{s}_{12}, \quad \mathbf{v}^{S_1^*} = u_1\mathbf{n}_1 + u_2\mathbf{n}_3 - u_3\mathbf{s}_{12} \times \left(\frac{l_1}{2}\mathbf{s}_{11}\right) \tag{39}$$

$$\omega^{M_2} = 0, \quad \mathbf{v}^{M_2^*} = u_4\mathbf{n}_1 + u_5\mathbf{n}_2 \tag{40}$$

$$\omega^{2} = -u_6\mathbf{s}_{22}, \quad \mathbf{v}^{*_2} = u_4\mathbf{n}_1 + u_5\mathbf{n} - u_6\mathbf{s}_{22} \times \left(\frac{l_2}{2}\mathbf{s}_{21}\right) \tag{41}$$

$$\omega^{M_3} = 0, \quad \mathbf{v}^{M_3^*} = u_7\mathbf{n}_1 + u_8\mathbf{n}_2 \tag{42}$$

$$\omega^{S_3} = -u_9\mathbf{s}_{32}, \quad \mathbf{v}^{S_3^*} = u_7\mathbf{n}_1 + u_8\mathbf{n}_3 - u_9\mathbf{s}_{32} \times \left(\frac{l_3}{2}\mathbf{s}_{31}\right) \tag{43}$$

$$\omega^{K} = u_{13}\mathbf{k}_1 + u_{14}\mathbf{k}_2 + u_{15}\mathbf{k}_3, \quad \mathbf{v}^{K^*} = u_{10}\mathbf{n}_1 + u_{11}\mathbf{n}_2 + u_{12}\mathbf{n}_3 \tag{44}$$

Next, note that the velocities of points P_i and S_i^e (i=1,2,3) can be expressed by:

$$\mathbf{v}^{P_2} = \mathbf{v}^{K^*} + \omega^{K} \times \mathbf{p}^{K^*P_2} = u_{10}\mathbf{n}_1 + u_{11}\mathbf{n}_2 + u_{12}\mathbf{n}_3 + r(u_{15}\mathbf{k}_2 - u_{14}\mathbf{k}_3) \tag{45}$$

$$\mathbf{v}^{S_2^e} = \mathbf{v}^{M_2^*} + \omega^{S_2} \times \mathbf{p}^{M_2^*S_2^e} = (u_4 + l_2u_6\sin q_6)\mathbf{n}_1 + u_5\mathbf{n}_2 + l_2u_6\cos q_6\mathbf{n}_3 \tag{46}$$

etc. In order to make the system move as planned, points P_1 and S_1^e, and similarly, points P_2 and S_2^e, as well as points P_3 and S_3^e, must coincide, say at $t = 0$, respectively, and, thereupon, move with equal velocities. That is,

$$\mathbf{v}^{P_1} = \mathbf{v}^{S_1^e} \tag{47}$$

$$\mathbf{v}^{P_2} = \mathbf{v}^{S_2^e} \tag{48}$$

$$\mathbf{v}^{P_3} = \mathbf{v}^{S_3^e} \tag{49}$$

Substituting Eqs. (45) and (46) into Eq. (48) gives rise to the following three scalar equations:

$$u_{10} - u_4 - l_2s_6u_6 - r(s_{13}s_{15} + s_{14}c_{13}c_{15})u_{14} + r(s_{15}c_{13} - s_{13}s_{14}c_{15})u_{15} = 0 \tag{50}$$

$$u_{11} - u_5 + r(c_{13}c_{15} + s_{13}s_{14}s_{15})u_{15} + r(s_{13}c_{15} - s_{14}s_{15}c_{13})u_{14} = 0 \tag{51}$$

$$u_1 - l\,c\,u + rs_{13}c_{14}u_{15} - rc_{13}c_{14}u_{14} = 0 \tag{52}$$

where $s_{13} \hat{=} \sin q_{13}$ and $c_{14} \hat{=} \cos q_{14}$ etc. These equations, along with six additional equations obtained similarly from Eqs. (47) and (49), can be solved for $u_1, ..., u_9$ in terms of $u_{10}, ..., u_{15}$, and arranged as follows:

$$u_i = \sum_{j=10}^{15} W_{ij}u_j \qquad (i = 1, \blacksquare, 9) \tag{53}$$

where W_{ij} $(i = 1, 2,...,9;\ j = 10, ..., 15)$ are functions of $q_1, ..., q_{15}$. Using the constraint equations, Eq. (53), to eliminate $u_1, ..., u_9$ from Eqs. (38) - (44), one is in a position to form six dynamic equations, governing the motion of the system in N. These equations can be cast in a matrix form, as follows:

$$\mathbf{M}\dot{\mathbf{u}} + \mathbf{C}\mathbf{u} + \mathbf{F} + \mathbf{G} = \mathbf{0} \tag{54}$$

where $\dot{\mathbf{u}} \hat{=} [\dot{u}_{10} \quad \cdots \quad \dot{u}_{15}]^T$, $\mathbf{M}$ is a 6×6 mass matrix, $\mathbf{C}$ is a 6×1 centrifugal - Corriolis matrix, and $\mathbf{F}$ and $\mathbf{G}$ are 6×1 matrices associated with control forces and gravitational forces. Their elements can be identified after note is taken of the fact that the forces acting on M_i^*, S_i^* $(i = 1,2,3)$ and K^* are

$$\mathbf{F}^{M_1^*} = F_1\mathbf{n}_1 + F_2\mathbf{n}_2 - M_{M_1}g\mathbf{n}_3 \tag{55}$$

$$\mathbf{F}^{M_2^*} = F_3\mathbf{n}_1 + F_4\mathbf{n}_2 - M_{M_2}g\mathbf{n}_3 \tag{56}$$

$$\mathbf{F}^{M_3^*} = F_5\mathbf{n}_1 + F_6\mathbf{n}_2 - M_{M_3}g\mathbf{n}_3 \tag{57}$$

$$\mathbf{F}^{S_1^*} = -M_{S_1}g\mathbf{n}_3, \quad \mathbf{F}^{S_2^*} = -M_{S_2}g\mathbf{n}_3, \quad \mathbf{F}^{S_3^*} = -M_{S_3}g\mathbf{n}_3 \tag{58)-(60}$$

$$\mathbf{F}^{K^*} = -M_K g\mathbf{n}_3 \tag{61}$$

where $F_1, ..., F_6$ are control forces components, M_{M_i}, M_{S_i} $(i = 1,2,3)$ and M_K are the masses of M_i, S_i (i=1,2,3) and K, g is the gravitational acceleration and $\mathbf{F} \hat{=} [F_1 \quad \cdots \quad F_6]^T$.

In summary, Eq. (54) can be solved, in conjunction with Eqs. (53) and (34) - (37), for $u_{10},...,u_{15}$ (and $u_1,...,u_9$) and $q_1, ..., q_{15}$, given initial conditions $q_1(0), ..., q_{15}(0)$, $u_{10}(0),..., u_{15}(0)$ and $F_1(t), ..., F_6(t)$.

It should be mentioned that similar to the known serial manipulator dynamic equation, Eq. (54) is the dynamic equation of the parallel manipulator counterpart.

Suppose now one wishes to solve for $F_1, ..., F_6$ - needed to bring about a desired motion of the system in N (the inverse problem). Then one may proceed as follows:

a. Define $u_{10}(t), ..., u_{15}(t)$ (the "desired motion").

b. Solve Eq. (53) for $u_1, ..., u_9$, and use $u_1...u_{15}$ in Eqs. (34) - (37) to obtain $q_1, ..., q_{15}$.

c. Find $\dot{u}_{10}(t),..., \dot{u}_{15}(t)$.

d. Solve Eq. (54) for $\mathbf{F}$ using $\dot{u}_{10} \ldots \dot{u}_{15}$, $u_{10} \ldots u_{15}$ and $q_1 \ldots q_{15}$.

If $q_{10}(t),\ldots, q_{15}(t)$ are given rather than $u_{10}(t),\ldots, u_{15}(t)$, then one starts with the evaluation of $u_{10}, \ldots, u_{15}$ using Eq. (34) (for $i = 10, 11, 12$) and (35) - (37). Then one may proceed in accordance with steps b - d above.

5.2 Dynamic simulation results

Simulation results of three types of parallel robots are given below: a) planarly actuated robot, b) a variation of the planary actuated robot where the joints order is reversed, i.e., spherical joints are attached to the motors and revolute joints to the moveable platform, and c) 3-3 Stewart platform.

Two trajectories were choosen: translation of 0.2 m in a constant velocity of 0.2 m/sec (Figs. 8a-8b) and rotation of 80 degrees about a Z axis in a constant angular velocity of 80 degrees/sec (Figs. 8c-8e).

Figs. 8f and 8g compare the maximum forces at the motors of the different robots needed to perform the above trajectories. This figures demonstrates the advantage of the planarly actuated robots. In both trajectories the force at the motors are considerably smaller that the commonly used Stewart platform (the same was evident for the 3-6 configuration).

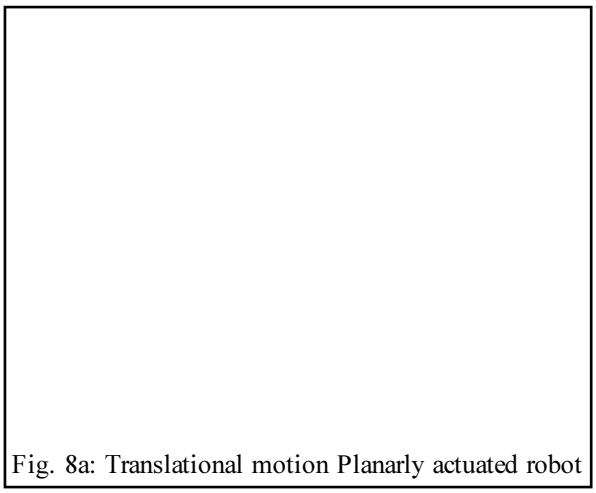

Fig. 8a: Translational motion Planarly actuated robot

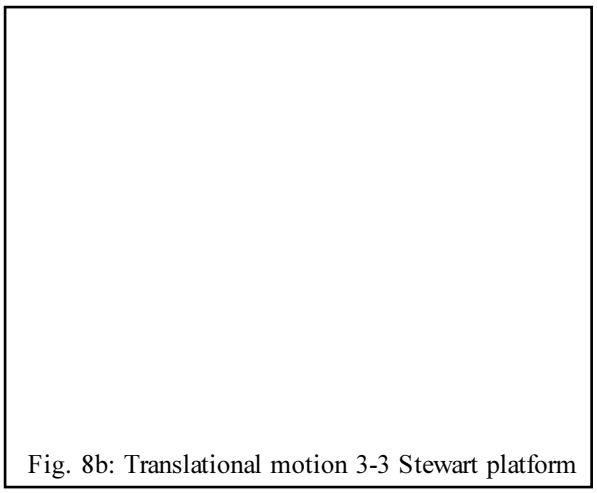

Fig. 8b: Translational motion 3-3 Stewart platform

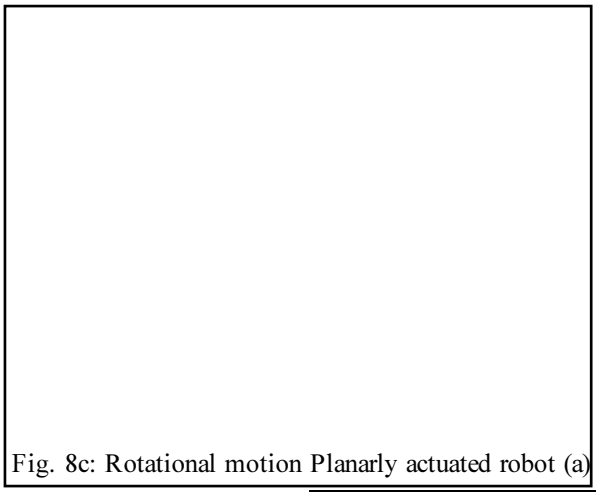

Fig. 8c: Rotational motion Planarly actuated robot (a)

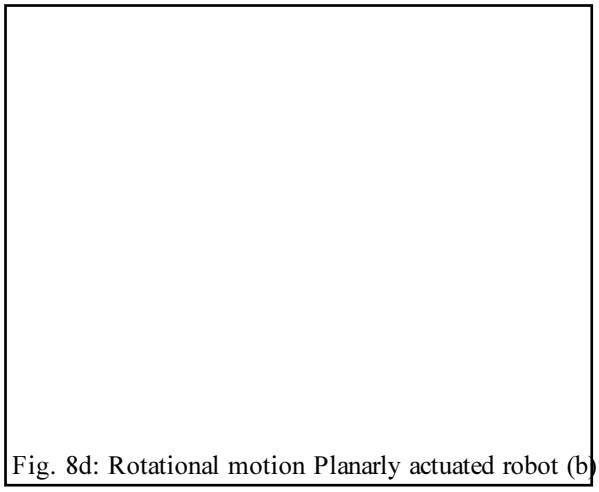

Fig. 8d: Rotational motion Planarly actuated robot (b)

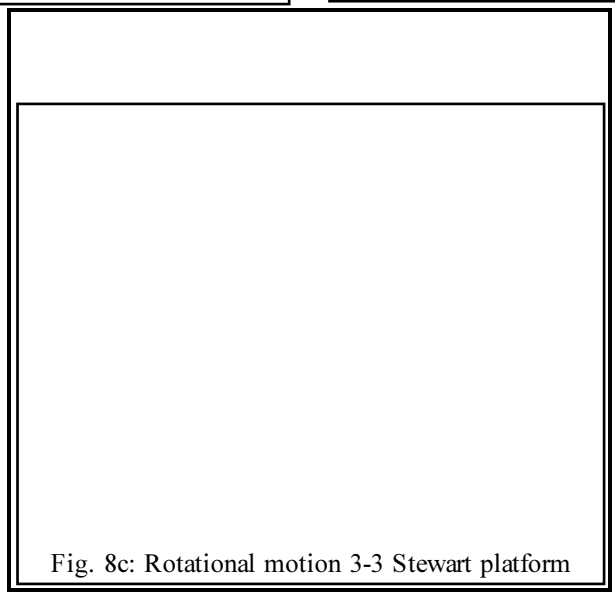

Fig. 8c: Rotational motion 3-3 Stewart platform

Fig. 8f: Translational motion largest motor force

Fig. 8g: Rotational motion largest motor force

Fig. 8: Dynamic simulation Results

6. THE EXPERIMENTAL SYSTEM

The configuration we used for the experimental system is shown in Fig. 2. This structure employs one spherical and one revolute joint at each one of the three links' end. The radius of the moveable platform is 60 mm and the length of the fixed length links is 200 mm. The motors used were Northern Magnetic's planar motor controlled by Motion Science's two axes controllers and connected to an IBM PC computer. Figs. 9 and 10 show the experimental system and a close view of the mechanism structure, respectively.

Fig. 9: The stationary platform and the robot

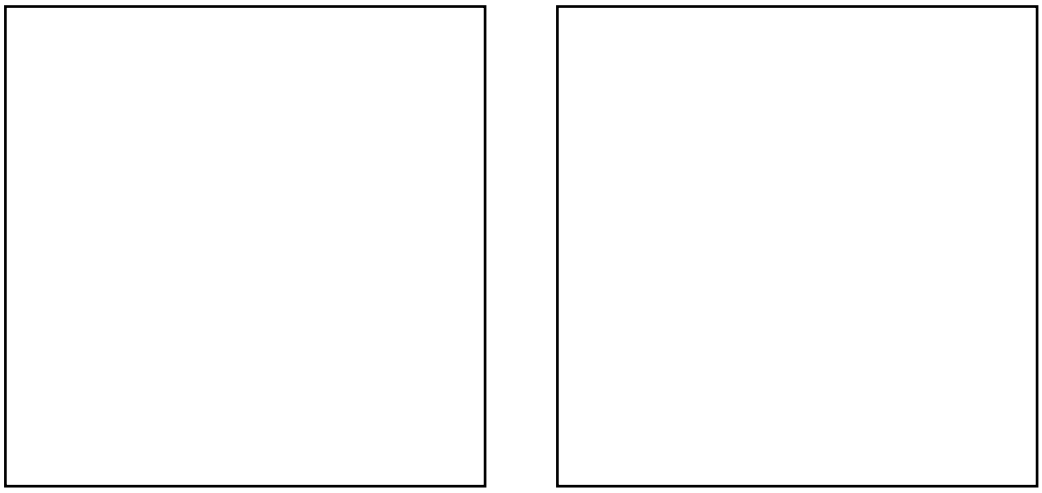

Fig. 10: The robot structure

7. THE SYSTEM PERFORMANCES

This simple robot structure, that has only seven moving parts, has a work volume which is limited only by the size of the stationary platform - 0.93 X 0.66 m in our design. It is well known that one of the major parallel robots' drawbacks is their limited work volume. The work volume is restricted by joint angles, link extensions limitations and by the interference between links. In our case, joint angles limitations and link interferences still exist, but there are no link extensions limitations since they are of fixed length. Additionaly, since the size of the stationary platform and not the dimensions of the moving parts determines its work volume, there is no common basis for comparison of its work volume with that of conventional parallel robots. Nevertheless, when considering only moving parts, the work volume of this robot (Fig. 11) is roughly one order of magnitude larger than a similar sized typical six-link Stewart platform (see [Stoughton and Arai, 1993; Wang and Masory, 1993]). The same is evident for orientational range. Pitch and yaw are about 100 degrees (and can easily be increased by redesigning the joints at the moveable platform) with roll reaching 300 degrees, if singular points are avoided, and close to 180 degrees, if singular points are considered.

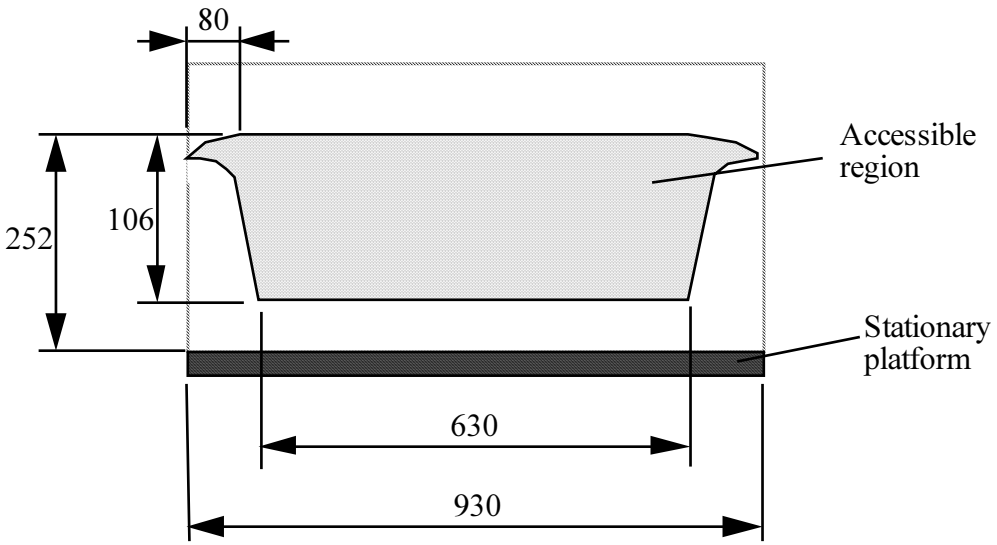

Fig. 11: Work volume cross section along the stationary platform long axis (dimensions in mm).

For the second version of the planarly actuated robot there is no singular point at ±90 degrees roll rotation and, theoretically, the rotational motion is unlimited.

The planar motor's maximum velocity is about 1 m/sec at about 13 N per axis force with each motor weighing 450 gr. Since the robot mass in our design was only 673 gr, the acceleration of the robot without payload is about half the acceleration of the motors alone.

The micro step resolution of the planar motors is 2.5 μm. Because of the mechanism structure, the repeatability in a planar motion of the moveable platform is the sum of the motor resolution and the clearance of the spherical joint (commonly less than 0.01 mm).

From computational point of view the simple inverse kinematics algorithm, which contains only 18 additions and substructions, 24 multiplications and divisions, and 6 trigonometric functions, allows a real time control with cycle time of considerably below 1 ms.

8. DISCUSSIONS AND CONCLUSIONS

Kinematics, dynamics and construction of a planarly actuated parallel robot is described in this paper. Both the forward and the inverse kinematics algorithms are simpler than the commonly used parallel robots due to only three moving links and the uncoupled planar motion of the motors. For the dynamic analysis, Kane's method was used in its general form and led to a set of equations from which both the inverse and the forward dynamics of different types of parallel robots can easily be obtained. This algorithm was used to simulate four different types of parallel robots - two versions of the planarly actuated robots, and the 3-3 and 6-3 Stewart platform.

Simulation results show the advantage of the planarly actuated robot in terms of work volume and fewer number of singular points. A mathematical derivation of the singular configurations of these types of robot which led to the same result, is the subject of a separate paper. Also, it was found that the variation of the planarly actuated robot with spherical joint at the motor side end, enables even larger work volume. Results of dynamic simulation show clearly the advantage of the planarly actuated robot in several paths. Much smaller forces are needed compare to a similar-sized Stewart platform both in translational and rotational motion.

The experimental model exhibits the simple robot design due to very few moving parts. The simple structure does not diminish its performances. On the contrary, it increases considerably its work volume, simplifies the kinematic solution and makes the robot very simple to construct. We believe that this type of parallel robot is very attractive for several industrial (e.g. assembly) applications as well as and non-industrial (e.g. medical) applications due to its unique combination of large work volume with high accuracy.

REFERENCES

1. Baiges I. J., and Duffy J., "Dynamic Modeling of Parallel Manipulators", *Proceedings of The 1996 ASME Design Engineering Technical Conferences and Computers in Engineering Conference*, August 18-22, 1996.
2. Ben-Horin R., and Shoham M., "Construction of a Six-Degrees-of-Freedom Parallel Manipulator with Three Planarly Actuated Links", *Proceedings of The 1996 ASME Design Engineering Technical Conferences and Computers in Engineering Conference*, August 18-22, 1996.
3. Chen N. X., and Song S. M., "Direct Position Analysis of the 4-6 Stewart Platforms", *ASME Conference on Robotics, Spatial Mechanisms, and Mechanical Systems*, DE-Vol. 45, 1992.
4. Do W. Q. D., and Yang D. C. H. , "Inverse Dynamic Analysis and Simulation of a Platform Type of Robot", *Journal of Robotic Systems*, Vol. 5, No. 3, pp. 209-227, 1988.
5. Gosselin C. M., "Parallel Computational Algorithm for the Kinematics and Dynamics of Planar and Spatial Parallel Manipulators", *AMSE Journal of Dynamic Systems, Measurement, and Control*, Vol. 118, pp. 22-28, 1996.
6. Hunt K. H., "Structural Kinematics of In-Parallel-Actuated Robot Arms," *AMSE Journal of Mechanisms, Transmissions and Automation in Design*, Vol. 105, No. 4, pp. 705-712, 1983.
7. Innocenti C., and Parenti-Castelli V., "A Novel Numerical Approach to the Closure of the 6-6 Stewart Platform Mechanism," *Proceedings of the 1991 IEEE International Conference on Robotics and Automation*, pp. 851-855, 1991.

8. Kane T. R., Likins P.W., and Levinson D. A., "Spacecraft Dynamics", *McGraw-Hill Book Company*, 1983.
9. Innocenti C., and Parenti-Castelli V., "Exhaustive Enumeration of Fully Parallel Kinematic Chains," *AMSE Conference on Dynamic Systems and Control*, DSC-Vol. 55-2, pp. 1135-1141,1994.
10. Lin W., Duffy J., and Griffs M., "Forward Displacement Analysis of the 4-4 Stewart Platforms", *Proceedings of the 1990 ASME Design Technical Conference,* DE-Vol. 25, pp. 263-269, 1990.
11. Lin W., Crane C. D., and Duffy J., "Close-Form Forward Displacement Analysis of the 4-5 In-Parallel Platforms", *ASME Conference on Robotics, Spatial Mechanisms, and Mechanical Systems*, DE-Vol. 45, 1992.
12. Liu K., Lewis F., Lebret G., and Taylor D., "The Singularities and Dynamics of a Stewart Platform Manipulator", Journal of Intelligent and Robotic Systems, Vol. 8, pp. 287-308, 1993.
13. Merlet J.-P., "Parallel Manipulators: State of the Art and Perspectives," *Advanced Robotics*, Vol. 8, pp. 589-596, 1994.
14. Nanua P., Waldron K. J., and Murthy V., "Direct Kinematic Solution of a Stewart Platform," *IEEE Transactions on Robotics and Automation*, Vol. 6, No. 4, pp. 438-444, 1990.
15. Pang H., and Shahinpoor M., " Inverse Dynamics of a Parallel Manipulator", *Journal of Robotic Systems*, Vol. 11, No. 8, pp. 693-702, 1996.
16. Pierrot F., Fournier A., and Dauchez P., "Towards a Fully-Parallel 6 DOF Robot for High-Speed Applications," *Proceedings of the 1991 IEEE International Conference on Robotics and Automation*, pp. 566-571, 1991.
17. Salmon G., *Lessons Introductory to the Modern Higher Algebra*, Fifth Edition, New York: Chelsea, pp. 76-83, 1964.
18. Stewart D. "A Platform with Six Degrees of Freedom," *in Proc. Inst. Mech. Engr. (London)*, Vol. 180, No. 1, pp. 371-386, 1965.
19. Stoughton R. S., and Arai T., "A Modified Stewart Platform Manipulator with Improved Dexterity," *IEEE Transactions on Robotics and Automation*, Vol. 9, No. 2, pp. 166-173, 1993.
20. Tahmasebi F., and Tsai L. W., "On the stiffness of a Novel Six-Degrees-of-Freedom Parallel Minimanipulator ," *Journal of Robotic Systems*, Vol. 12, No. 12, pp. 845-856, 1995.
21. Tsai L. W., and Tahmasebi F., "Synthesis and Analysis of a New Class of Six-Degrees-of-Freedom Parallel Minipulators," *Journal of Robotic Systems*, Vol. 10, No. 5, pp. 561-580, 1993.
22. Tsai L. W., and Tahmasebi F., "Closed-Form Direct Kinematics Solution of a New Parallel Minimanipulator", *ASME Journal of Mechanical Design*, Vol. 116, pp. 1141-1147, 1994.

23. Waldron K. J., Raghavan M., and Roth B., "Kinematics of a Hybrid Series-Parallel Manipulation System," *ASME Journal of Dynamic Systems, Measurement and Control*, Vol. 111, No. 2, pp. 211-221, 1989.
24. Wang J., and Masory O., "Workspace Evaluation of Stewart Platforms," *Advanced Robotics*, Vol. 9, No. 4, pp. 443-461, 1993.
25. Zhang C. D.,and Song S. M. ," An Efficient Method for Inverse Dynamics of Manipulators Base on the Virtual Work Principle", *Journal of Robotic Systems*, Vol. 10, No. 5, pp. 605-627, 1993.
26. Zhiming J., "Dynamics Decomposition for Stewart Platforms", *ASME Journal of Mechanical Design*, Vol. 116, pp. 67-69, 1994.